https://doi.org/10.15407/ujpe68.9.577

M.A. HASAN, A.H. TAQI

Department of Physics, College of Science, University of Kirkuk
(Kirkuk, Iraq; e-mail: Malik.abdullah@uokirkuk.edu.iq)

PROTON AND NEUTRON PAIRING PROPERTIES WITHIN A MIXED VOLUME-SURFACE PAIRING TYPE USING THE HARTREE–FOCK–BOGOLYUBOV THEORY

This work aims at systematic investigations of the proton and neutron pairing properties and Fermi energies in the region from the proton drip-line to the neutron drip-line. In order to obtain a more accurate mass formula with the Skyrme (SKI3) force, the global descriptive power of the Skyrme–Hartree–Fock–Bogoliubov model for pairing properties is applied. Systematic Skyrme–HFB calculations with a mixed volume-surface pairing are carried out to study the ground-state proton pairing gap, neutron and proton pairing energies, and the neutron and proton Fermi energies for about 2095 even-even nuclei ranging from $2 \leqslant Z \leqslant 110$ *to* $2 \leqslant N \leqslant 236$*. The calculated values of proton pairing gaps are compared with experimental data, by using the difference-point formulas* $\Delta^{(3)}$*,* $\Delta^{(4)}$*, and* $\Delta^{(5)}$*, and compared with the proton pairing gap in the Lipkin–Nogami model. It is shown that the Skyrme (SKI3) force with the mixed volume-surface pairing can be successfully used for describing the ground-state proton pairing gap, proton and neutron pairing energies, and proton and neutron Fermi properties of the investigated nuclei, in particular, the neutron-rich nuclei and the exotic nuclei near the neutron drip-line. On the other hand, the calculated proton pairing gap shows the acceptable agreement with the available experimental values of the proton pairing gap with the use of the difference-point formulas* $\Delta^{(3)}$*,* $\Delta^{(4)}$*, and* $\Delta^{(5)}$ *and with the data of the Lipkin–Nogami model over the whole nuclear chart.*

K e y w o r d s: Skyrme–Hartree–Fock–Bogoliubov theory (SHFB), proton pairing gap, proton and neutron pairing energies, proton and neutron Fermi energies.

1. Introduction

The pairing correlations can be considered as a major ingredient in describing the nuclear ground-state properties for the finite nuclei. It is based on the so-called BCS approximation, which was introduced by Bardeen–Cooper–Schrieffer in superconductivity theory in metals. The nuclear pairing correlations were established, for the first time, about 60 years ago [1, 2]. Till today, the study of the structure of exotic nuclei, which are lying away from the beta-stability line and close to the proton or neutron drip-line, plays an important role in describing and understanding the properties of low-lying nuclei in the ground-state. Those nuclei (exotic or halo nuclei) which are lying in the regions far from the β-stability line have attracted a wide attention and represent one of the most open and active areas of research in the field of nuclear physics, both theoretically and experimentally [3–7].

To describe the nuclear ground-state properties such as the pairing gap and the pairing energy of ex-

C i t a t i o n: Hasan M.A., Taqi A.H. Proton and neutron pairing properties within a mixed volume-surface pairing type using the Hartree–Fock–Bogolyubov theory. *Ukr. J. Phys.* **68**, No. 9, 577 (2023). https://doi.org/10.15407/ujpe68.9.577.

Ц и т у в а н н я: Хасан М.А., Такі А.Х. Властивості змішаного об'ємно-поверхневого двійкування протонів і нейтронів в теорії Хартрі–Фока–Боголюбова. *Укр. фіз. журн.* **68**, №9, 579 (2023).

otic nuclei, especially on those regions on the neutron-rich side of the β-stability valley, an appropriate theoretical framework is needed to describe these exotic regions [8, 9]. The Hartree–Fock–Bogoliubov (HFB) approach is a good theoretical framework to study and describe the nuclear pairing correlations [10–16]. In general, the HFB theory consists of two parts: first, the self-consistent mean-field from the Hartree–Fock (HF) theory which describes the long-range part as the particle-hole (p-h) channel used in closed-shell configurations, and the second part is the pairing correlations obtained from the Bardeen–Cooper–Schrieffer (BCS) theory [17] of superconductivity in metals, which describes the short-range part as the particle-particle (p-p) channel used in open-shell configurations. By depending on the two channels, the density matrix (ρ_{ij}) and the pairing tensor density (κ_{ij}) can be used to characterize the nuclear system. The two parts were unified and achieved in a general HFB formalism using a variational principle [18, 19].

In the previous paper [20], we have studied the ground-state binding energy, two-neutron separation energy (S_{2n}), quadrupole deformation parameter (β_2), charge radii, neutron and proton rms radii, and neutron pairing gaps of the whole nuclear chart. Our previous study [20] with the Skyrme (SKI3) force showed success in describing the ground-state properties by comparing the calculated results with the experimental data and other models such as the Finite Range Droplet Model (FRDM), Relativistic Mean-Field (RMF) model, and HFB calculations based on the D1S Gogny force. The authors S.A. Changizi, *et al.* in Refs. [21, 22] presented a systematic study of the neutron pairing gaps predicted by HFB calculations with the Skyrme (SLy4) parameter with the different volume, surface, and mixed volume-surface pairing types. Thus, in order to make a comprehensive perception to describe the nuclear landscape with different Skyrme forces, we will investigate the properties of the proton pairing gap, proton and neutron pairing energies, and neutron and proton Fermi energies for about 2095 even-even nuclei with (He) $2 \leqslant Z \leqslant 110$ (Ds) over a wide range of isotopes starting from the neutron number $N = 2$ to $N = 236$ ($4 \leqslant A \leqslant 346$). The investigated properties of the whole nuclear chart are based on the HFB theory using Skyrme (SKI3) force [23] with a mixed volume-surface pairing type. The calculated results for the proton pairing gap have been compared with the proton pairing gap of the available experimental data by the difference-point formulas $\Delta^{(3)}$, $\Delta^{(4)}$, and $\Delta^{(5)}$, and also compared with the proton pairing gap obtained in the Lipkin–Nogami model (Δ_p^{LN}) data [24–26] to show the consistence and the validity of our calculated results. It is necessary to mentioned that the studies of the whole nuclear chart with the Skyrme (SKI3 parameter are few somewhat in the nuclear structure, for this reason; this force (SKI3) was chosen in this study, because it gives a good predictions and results in describing the nuclear structure (see Ref. [20], for example).

The structure of this paper is organized as follows. In Sec. 2, a brief theoretical framework of the HFB approach is presented. The numerical details of this study are given in Sec. 3. The results and discussion are given in Sec. 4. Finally, the conclusions are presented in Sec. 5.

2. The HFB Formalism

The HFB approach has been extensively discussed in the literature [10–12], and we will only briefly introduce it here. In the standard HFB formalism, the two-body Hamiltonian of a system of fermions can be expressed in terms of a set of annihilation and creation operators $(c, c^\dagger)$ [10, 11]:

$$H = \sum_{n_1 n_2} e_{n_1 n_2} c^\dagger_{n_1} c_{n_2} + \\ + \frac{1}{4} \sum_{n_1 n_2 n_3 n_4} \bar{v}_{n_1 n_2 n_3 n_4} c^\dagger_{n_1} c^\dagger_{n_2} c_{n_4} c_{n_3}, \tag{1}$$

where the first term corresponds to the kinetic energy, and $\bar{v}_{n_1 n_2 n_3 n_4} = \langle n_1 n_2 | V | n_3 n_4 - n_4 n_3 \rangle$ is the matrix element of the two-body interaction between antisymmetrized two-particle states. The HFB ground-state wave function $|\Phi\rangle$ is defined as the quasiparticle vacuum $\alpha_k |\Phi\rangle = 0$, where the quasiparticle operators $(\alpha, \alpha^\dagger)$ are connected to the original particle operators via a linear Bogoliubov transformation [10, 11]:

$$\left.\begin{aligned} \alpha_k &= \textstyle\sum_n (U^*_{nk} c_n + V^*_{nk} c^\dagger_n), \\ \alpha^\dagger_k &= \textstyle\sum_n (V_{nk} c_n + U_{nk} c^\dagger_n), \end{aligned}\right\} \tag{2}$$

which can be rewritten in the matrix form as:

$$\begin{pmatrix} \alpha \\ \alpha^\dagger \end{pmatrix} = \begin{pmatrix} U^\dagger & V^\dagger \\ V^T & U^T \end{pmatrix} \begin{pmatrix} c \\ c^\dagger \end{pmatrix}. \tag{3}$$

The matrices U and V satisfy the relations [10, 11]:

$$\left.\begin{aligned} &U^{\dagger}U + V^{\dagger}V = I,\\ &UU^{\dagger} + V^{*}V^{T} = I,\\ &U^{T}V + V^{T}U = 0,\\ &UV^{\dagger} + V^{*}U^{T} = 0. \end{aligned}\right\} \tag{4}$$

In terms of the normal density ρ and pairing tensor κ, the one-body density matrices are:

$$\left.\begin{aligned} \rho_{n\acute{n}} &= \langle\Phi|c^{\dagger}_{\acute{n}}c_{n}|\Phi\rangle = (V^{*}V^{T})_{n\acute{n}},\\ \kappa_{n\acute{n}} &= \langle\Phi|c_{\acute{n}}c_{n}|\Phi\rangle = (V^{*}U^{T})_{n\acute{n}}. \end{aligned}\right\} \tag{5}$$

The expectation value of Eq. (1) can be expressed in an energy functional as [10, 11]:

$$E[\rho,\kappa] = \frac{\langle\Phi|H|\Phi\rangle}{\langle\Phi|\Phi\rangle} = \mathrm{Tr}\left[\left(e + \frac{1}{2}\Gamma\right)\rho\right] - \frac{1}{2}\mathrm{Tr}\left[\Delta\kappa^{*}\right], \tag{6}$$

where the self-consistent term is:

$$\Gamma_{n_1n_3} = \sum_{n_2n_4}\bar{v}_{n_1n_2n_3n_4}\rho_{n_4n_2}, \tag{7}$$

and the pairing field term is:

$$\Delta_{n_1n_2} = \frac{1}{2}\sum_{n_3n_4}\bar{v}_{n_1n_2n_3n_4}\kappa_{n_3n_4}. \tag{8}$$

The variation of the energy (Eq. (6)) with respect to ρ and κ leads to the HFB equations [10, 11]:

$$\begin{pmatrix} e+\Gamma-\lambda & \Delta \\ -\Delta^{*} & -(e+\Gamma)^{*}+\lambda \end{pmatrix}\begin{pmatrix} U \\ V \end{pmatrix} = E\begin{pmatrix} U \\ V \end{pmatrix}, \tag{9}$$

where the Lagrange multiplier λ has been introduced to fix the correct average particle number, and Δ denotes the pairing potential.

3. Numerical Details

In this paper, the ground-state properties of the even-even nuclei have been investigated by using the code HFBTHO (v2.00d) [12] with the Skyrme (SKI3) force [23], which utilizes the axial Transformed Harmonic Oscillator (THO) single-particle basis to expand quasiparticle wave functions. It iteratively diagonalizes the HFB Hamiltonian based on generalized Skyrme-like energy densities and a zero-range pairing interaction until a self-consistent solution is found [11, 12].

The calculations were performed with a mixed volume-surface pairing type using a cutoff quasiparticle energy $E_{\mathrm{cut}} = 60$ MeV, which means that all the quasiparticles with the energy lower than the cutoff are taken into account in the calculations of the densities. The Harmonic Oscillator (HO) basis was characterized by the oscillator length $b = -1.0$ fm, which means that the code automatically sets b_0 by using the relation for the HO frequency [12]:

$$b_0 = \sqrt{\hbar/m\omega}, \tag{10}$$

where $\hbar\omega = 1.2 \times 41/A^{1/3}$. In order to obtain a more accurate results, the number of oscillator shells (the principal number of oscillator shells N) taken into account was $N_{\max} = 20$ shells. The axial deformation parameter (β_2) of the basis was 0.2 (the deformation value 0.2 is a value that mediates the values of large and small deformations). The input data of the pairing strength in the code HFBTHO (v2.00d) in Eq. (11) for neutrons V_0^n and protons V_0^p have been used as a pre-defined pairing force depending on a standard value of each Skyrme force used in the code HFBTHO. In the case of the SKI3 force, the pairing strength value for neutrons $V_0^n = -357.23$ MeV and, for protons, $V_0^p = -388.56$ MeV. It is always assumed that the pairing force reads:

$$V^{n,p}_{\mathrm{pair}}(\mathbf{r}) = V_0^{n,p}\left(1 - \alpha\frac{\rho(\mathbf{r})}{\rho_c}\right)\delta(\mathbf{r} - \acute{\mathbf{r}}). \tag{11}$$

Where $\rho(\mathbf{r})$ is the local density, and ρ_c is the saturation density, fixed at $\rho_c = 0.16$ fm^{-3}, and the type of a pairing force defined by the parameter α, which can be volume, surface, or mixed volume-surface characteristics [12]. More about numerical details can be found in Refs. [20, 27].

4. Results and Discussion

In this section, the ground-state properties of the pairing and Fermi properties for about 2095 even-even nuclei with (He) $2 \leqslant Z \leqslant 110$ (Ds) over a wide range of isotopes starting from the neutron number $N = 2$ to $N = 236$ ($4 \leqslant A \leqslant 346$) will be investigated and discussed by using the skyrme–HFB theory with the mixed volume-surface zero-range pairing force interaction.

4.1. Proton pairing gap

The proton pairing gap can be expressed in the same way as in the neutron pairing gap, only by keeping

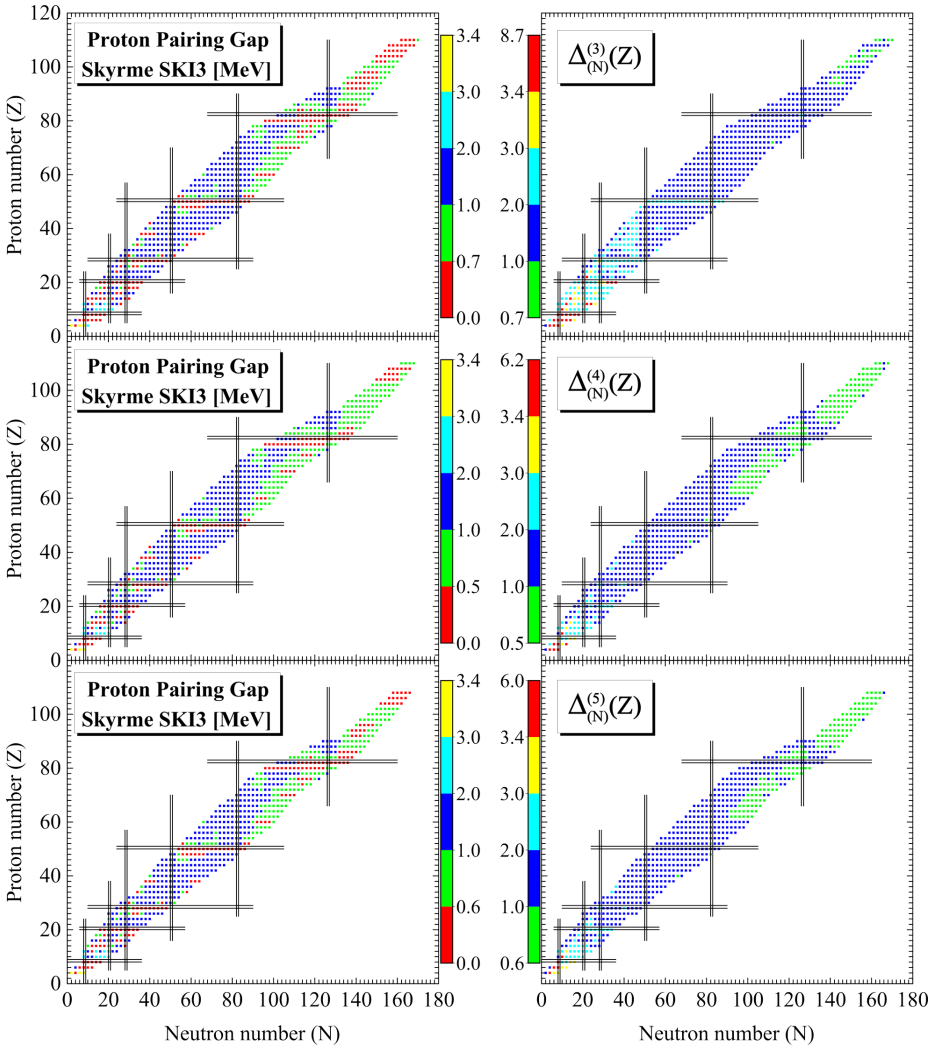

Fig. 1. (Color online) HFBTHO calculations with the mixed volume-surface pairing type for 759 even-even nuclei as a function of the proton (Z) and neutron (N) numbers: (left panel) the calculated proton pairing gap with Skyrme (SKI3) force, in comparison with the values of the experimental formulas $\Delta^{(3)}_N(Z), \Delta^{(4)}_N(Z)$ and $\Delta^{(5)}_N(Z)$ (right panel)

the neutron number (N) constant and varying the proton number (Z) around neighboring isotones. In Fig. 1 (left panel), the calculated results for 759 even-even nuclei concerning the proton pairing gap from $Z = 4$, $N = 2$ to $Z = 110$, $N = 170$ with Skyrme (SKI3) force have been plotted as a function of the proton (Z) and neutron (N) numbers and compared with the available experimental data of many finite-difference formulas which are often interpreted as a measurement of the empirical gap, as it seen in Fig. 1 (right panel). The three-point $\Delta^{(3)}_N(Z)$ formula is expressed as [28, 29]:

$$\Delta^{(3)}_N(Z) \equiv \frac{\pi_Z}{2}[BE(N, Z-1) + BE(N, Z+1) - \\ - 2BE(N, Z)]. \quad (12)$$

The four- $\Delta^{(4)}_N(Z)$ and five-point $\Delta^{(5)}_N(Z)$ formulas can be defined as [2, 28, 30–32]:

$$\Delta^{(4)}_N(Z) \equiv \frac{\pi_Z}{4}[BE(N, Z-2) + 3BE(N, Z) - \\ - 3BE(N, Z-1) - BE(N, Z+1)]. \quad (13)$$

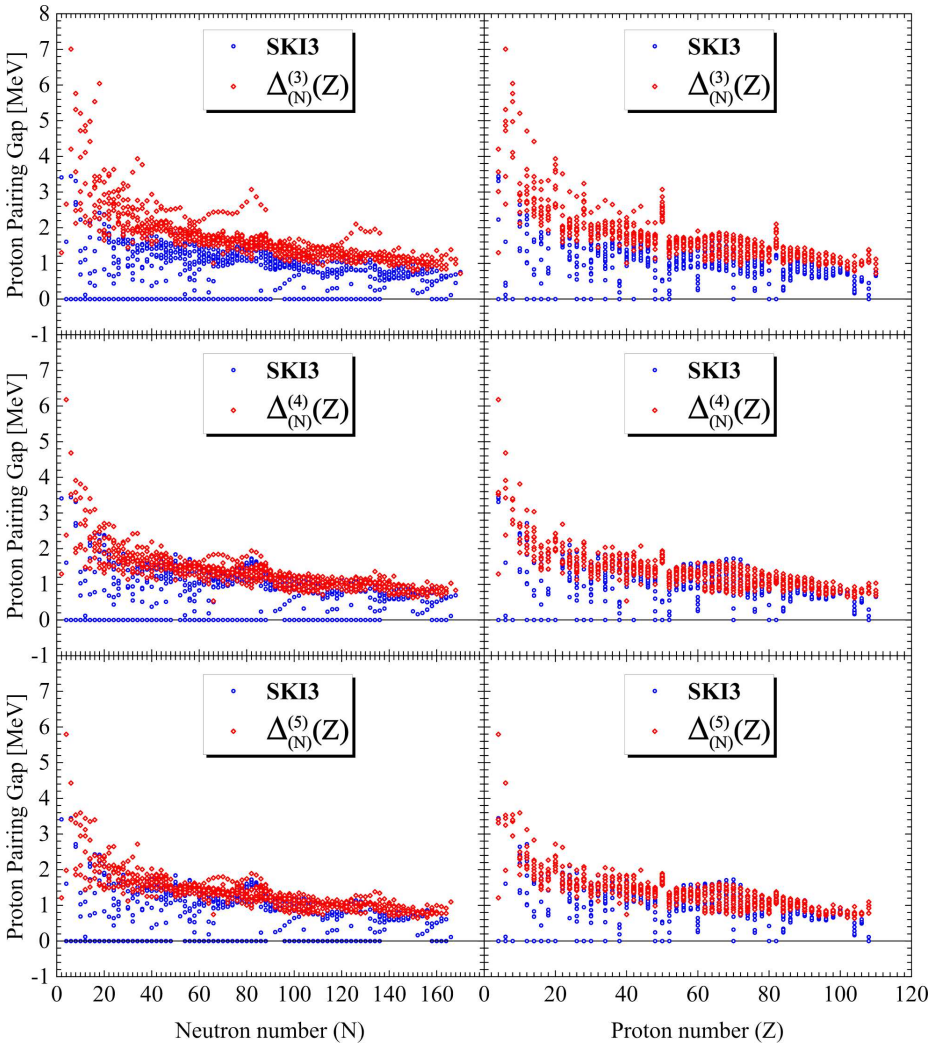

Fig. 2. (Color online) Skyrme SKI3-HFBTHO calculations of proton pairing gap with the mixed volume-surface pairing type for 759 even-even nuclei in comparison with the formulas $\Delta^{(3)}_N(Z)$, $\Delta^{(4)}_N(Z)$, and $\Delta^{(5)}_N(Z)$ values (left panel) as a function of the neutron number (N) and (right panel) as a function of the proton number (Z)

$$\Delta^{(5)}_N(Z) \equiv -\frac{\pi_Z}{8}[BE(N,Z+2)+6BE(N,Z)+$$
$$+BE(N,Z-2)-4BE(N,Z-1)-$$
$$-4BE(N,Z+1)]. \quad (14)$$

In Fig. 1 (left panel), the calculated results for the proton pairing gap with the SKI3 force are ranged from 0 MeV for many nuclei (for example, ^{40}Ca) up to the maximum value ≈3.44 MeV at $Z = 4$, $N = 6$ (^{10}Be), whereas the values of $\Delta^{(3)}_N(Z)$ are ranged between 0.748 MeV at $Z = 104$, $N = 150$ (^{254}Rf) up to the maximum value 8.72 MeV at $Z = 4$, $N = 4$ (^{8}Be). The values of $\Delta^{(4)}_N(Z)$ are ranged between 0.53 MeV at $Z = 40$, $N = 66$ (^{106}Zr) up to the maximum value 6.18 MeV at $Z = 4$, $N = 4$ (^{8}Be), and the values of $\Delta^{(5)}_N(Z)$ are ranged between 0.63 MeV at $Z = 104$, $N = 152$ (^{256}Rf) up to the maximum value 5.97 MeV at $Z = 4$, $N = 4$ (^{8}Be) as seen in Fig. 1 (right panel).

Figure 2 (left panel) shows the calculated proton pairing gap in comparison with the $\Delta^{(3)}_N(Z)$, $\Delta^{(4)}_N(Z)$, and $\Delta^{(5)}_N(Z)$ values as a function of the neutron

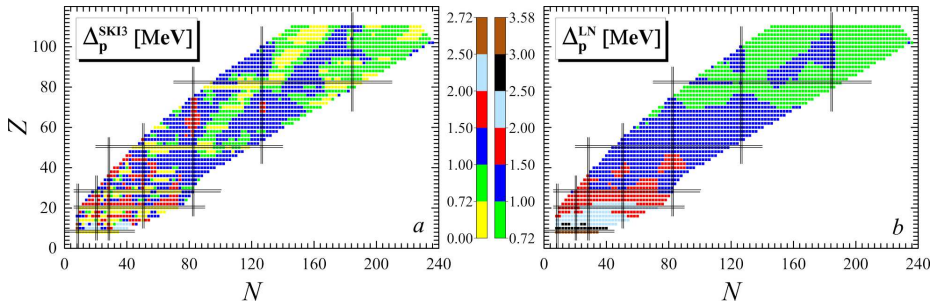

Fig. 3. (Color online) HFBTHO calculations with the mixed volume-surface pairing type for 2076 even-even nuclei as a function of the proton (Z) and neutron (N) numbers: (a) calculated proton pairing gap with the SKI3 force in comparison with the (b) proton pairing gap in the Lipkin–Nogami model [24]

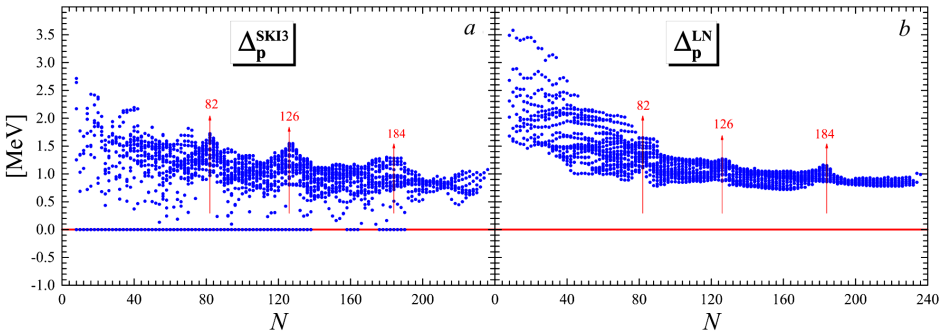

Fig. 4. (Color online) Same as Fig. 3, but as a function of the neutron number N only

number (N). The calculated results with the Skyrme (SKI3) force started with a high values at the light nuclei regions (from $Z = 2$, $N = 4$ to $Z = 20$, $N = 24$) and decreased as the number of neutrons increases. In general, the calculated results show the clear consistency with the values of $\Delta_N^{(3)}(Z)$, $\Delta_N^{(4)}(Z)$, and $\Delta_N^{(5)}(Z)$ formulas (especially with the $\Delta_N^{(4)}(Z)$ formula). The same behavior can be seen in Fig. 2 (right panel) which shows the calculated proton pairing gap in comparison with the $\Delta_N^{(3)}(Z)$, $\Delta_N^{(4)}(Z)$, and $\Delta_N^{(5)}(Z)$ values as a function of the proton number (Z). It is worth to mention that the values of the calculated proton pairing gap for most nuclei that have magic (or semimagic) numbers with Z, $N = 8, 20, 28, 50, 82$, and 126 found to be with a zero values, while the difference pairing gap formulas ($\Delta_N^{(3)}(Z)$, $\Delta_N^{(4)}(Z)$ and $\Delta_N^{(5)}(Z)$) do not have a zero values for the nuclei with magic (or semi-magic) numbers.

In Fig. 3, a, the calculated results for even-even proton pairing gaps (Δ_p^{SKI3}) with the SKI3 force have been plotted as a function of the proton (Z) and neutron (N) numbers and compared with the available data of the proton pairing gap (Δ_p^{LN}) in the Lipkin–Nogami model [24] as seen in Fig. 3, b. In Fig. 3, a, the calculated/measured values of Δ_p^{SKI3} for 2076 even-even nuclei from $Z = 8$, $N = 8$ (^{16}O) to $Z = 110$, $N = 236$ (^{346}Ds) are ranged from 0 MeV for many nuclei (for example, ^{56}Ni) up to the maximum value $\approx$2.72 MeV at $Z = 12$, $N = 8$ (^{20}Mg), whereas the values of Δ_p^{LN} are ranged between 0.72 MeV at $Z = 108$, $N = 160$ (^{268}Hs) up to the maximum value 3.58 MeV at $Z = 8$, $N = 10$ (^{18}O) as seen in Fig. 3, b. The values of Δ_p^{SKI3} in the regions with $8 \leqslant Z, N \leqslant 50$ are not so regular as in the same regions for Δ_p^{LN} values. However, the regions above $Z, N > 50$ (green and blue colors with 0.72 and 1 MeV $\leqslant \Delta_p^{\mathrm{SKI3}} \leqslant 1$ and 1.5 MeV, respectively) up to the end of the chart show the clear consistency with the values of Δ_p^{LN}, except for some small regions ($N \geqslant 82$) with red color ($1.5 \leftrightarrow 2$ MeV) that appear in Δ_p^{SKI3} chart and do not found in Δ_p^{LN} chart. Moreover, the large values of Δ_p^{SKI3} and Δ_p^{LN} are concentrated in the regions with light nuclei with $N \leqslant 43$, as is clear from

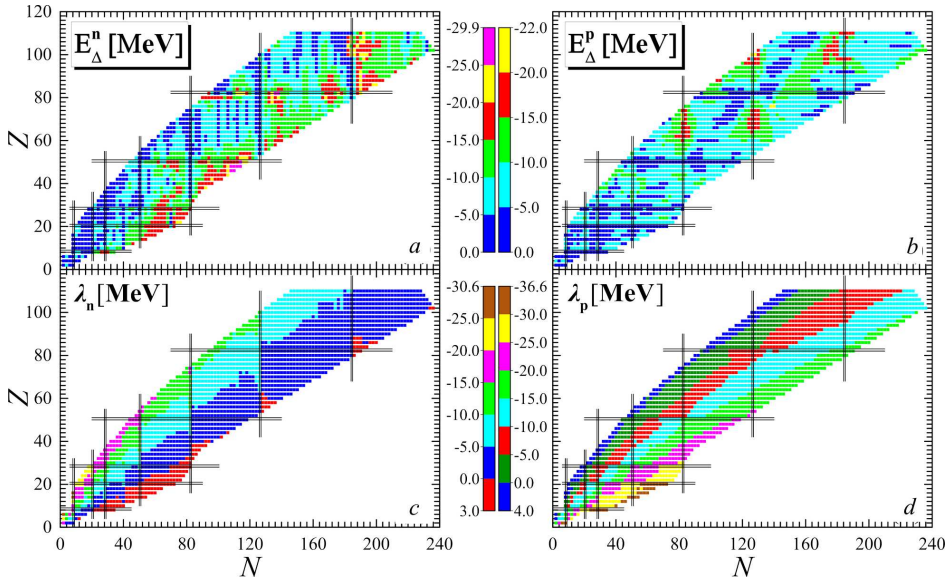

Fig. 5. (Color online) HFBTHO calculations with the mixed volume-surface pairing for 2095 even-even nuclei as a function of (Z) and (N): (a) and (b) are calculated neutron and proton pairing energies with Skyrme (SKI3) force, respectively, (c) and (d) are the calculated neutron and proton Fermi energies with the Skyrme (SKI3) force, respectively

Fig. 3, *a, b* for $\Delta_p^{\rm SKI3}$ and $\Delta_p^{\rm SKI3}$, respectively. Another note that follows from Fig. 3, *a* is that the values of the $\Delta_p^{\rm SKI3}$ for all the nuclei with the double magic or semimagic numbers ($Z = N = 2, 8, 20, ..., 184$) are $0 \to 0.72$ MeV as expected. This behavior is not found in proton pairing gap values in the Lipkin–Nogami model $\Delta_p^{\rm LN}$.

In Fig. 4, *a*, the calculated results for $\Delta_p^{\rm SKI3}$ with the SKI3 force have been plotted as a function of the neutron (N) number and compared with the available data of $\Delta_p^{\rm LN}$ in the Lipkin–Nogami model [24], as shown in Fig. 4, *b*. The values of $\Delta_p^{\rm SKI3}$ started with a large values in the regions of light nuclei and began to decrease toward the neutron drip-line as the neutron number increases for both the calculated results with $\Delta_p^{\rm SKI3}$ and the Lipkin–Nogami $\Delta_p^{\rm LN}$ data. The calculated results with $\Delta_p^{\rm SKI3}$ are not so regular as in the Lipkin–Nogami model with $\Delta_p^{\rm LN}$. The regions with the magic numbers ($N = 82, 126$ and 184) appear as peaks, as shown in Fig. 4, *a, b* for $\Delta_p^{\rm SKI3}$ and $\Delta_p^{\rm LN}$, respectively. Remarkably, the regions of those nuclei which located between the magic numbers have low values of $\Delta_p^{\rm SKI3}$ and $\Delta_p^{\rm LN}$ which is clearly seen as fluctuations in Fig. 4, *a, b* for $\Delta_p^{\rm SKI3}$ and $\Delta_p^{\rm LN}$, respectively.

4.2. Neutron and proton pairing energies and Fermi energy

The pairing energy and the Fermi energy are the important features in the description of the properties of nuclei. From the Fermi energy, we can obtain an important information, especially about the exotic nuclei near/at the neutron drip-line region by showing the boundaries of the nuclear landscape [25, 26, 33, 34].

The calculated results for the neutron pairing energy E_Δ^n [Fig. 5, *a*], proton pairing energy E_Δ^p [Fig. 5, *b*], neutron Fermi energy λ_n [Fig. 5, *c*], and proton Fermi energy λ_n [Fig. 5, *d*] using the mixed volume-surface pairing with Skyrme (SKI3) force have been plotted as a function of the proton (Z) and neutron (N) numbers. In Fig. 5, *a*, the calculated values of E_Δ^n for 2095 even-even nuclei from $Z = 2$, $N = 2$ (^{4}He) to $Z = 110$, $N = 236$ (^{346}Ds) are ranged from 0 MeV for many nuclei (for example, ^{4}He) up to the maximum value ≈ -29.888 MeV at $Z = 46$, $N = 110$ (^{156}Pd). The values of E_Δ^p are ranged between 0 MeV at $Z = 2$, $N = 2$ (^{4}He) up to the maximum value –21.992 MeV at $Z = 100$, $N = 126$ (^{226}Fm), as is seen in Fig. 5, *b*. The values of λ_n are ranged between –30.504 MeV at $Z = 6$, $N = 2$

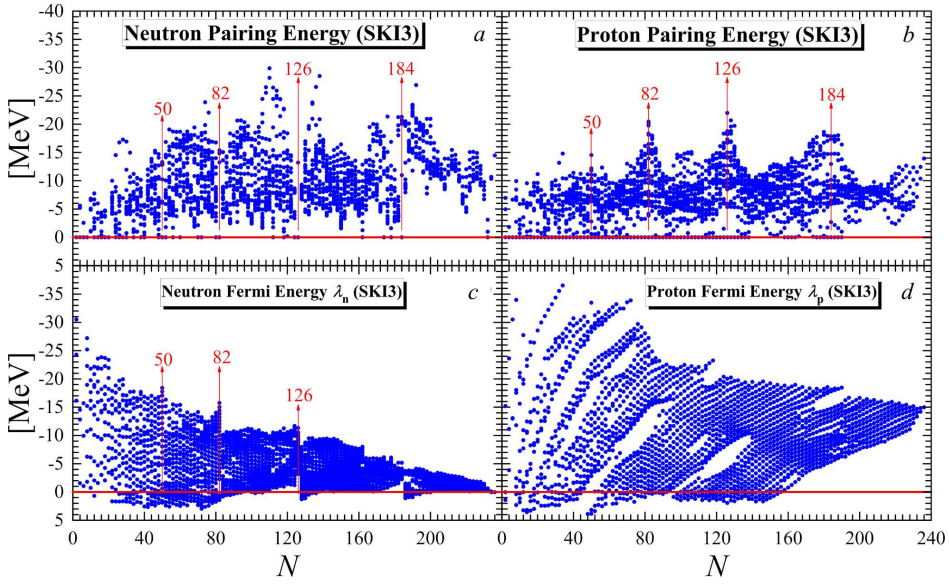

Fig. 6. (Color online) Same as Fig. 5, but as a function of the neutron number N only

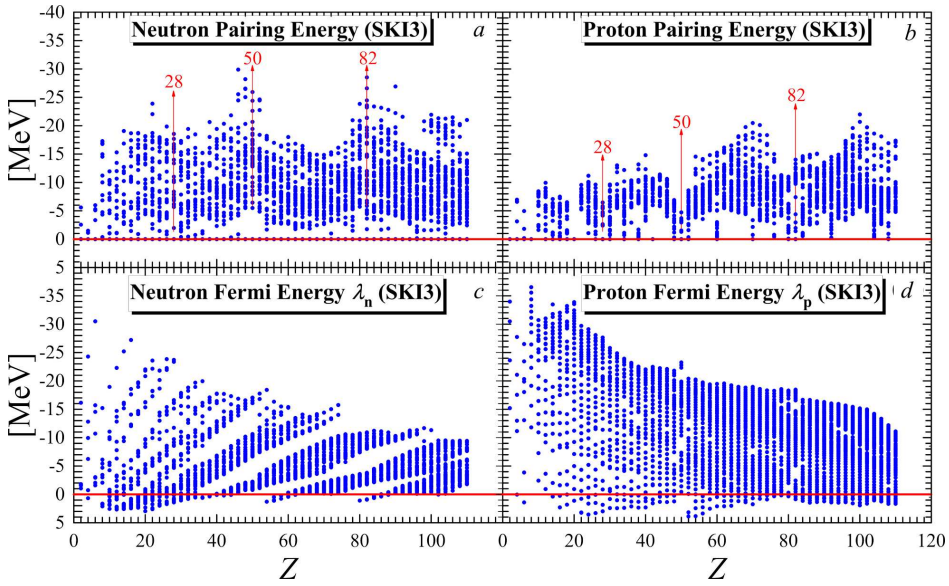

Fig. 7. (Color online) Same as Fig. 6, but as a function of the proton number Z only

(^{8}C) up to the maximum value 2.96 MeV at $Z = 20$, $N = 72$ (^{92}Ca), as is seen in Fig. 5, *c*, and the values of λ_p are ranged between –36.522 MeV at $Z = 8$, $N = 34$ (^{42}O) up to the maximum value 3.889 MeV at $Z = 52$, $N = 48$ (^{100}Te), as is seen in Fig. 5, *d*.

The calculated E^n_Δ, E^p_Δ, λ_n, and λ_p with the SKI3 force have been plotted as a function of the neutron (N) number, as is shown in Fig. 6, *a, b, c, d*, respectively. As can be seen from Fig. 6, *a*, the regions between the magic numbers ($N = 50, 82, 126$ and 184) have a large values of E^n_Δ, and appear as peaks. It should be mentioned that most nuclei with the neutron magic numbers have a E^n_Δ value close to the zero line (i. e., between $0 \to -0.5$ MeV). In contrast to the Fig. 6, *a*, the regions with the magic numbers ($N = 50, 82, 126$ and 184) have a large values of E^p_Δ

and appear as peaks, as is shown in Fig. 6, *b*. Remarkably, the regions of those nuclei which are located between the magic numbers have low values of E^p_Δ which is clearly seen as fluctuations in Fig. 6, *b*. The neutron Fermi energy λ_n in Fig. 6, *c* starts with large values at the regions of light nuclei. Then, as the neutron number begin to increase, the λ_n begin to decrease toward the neutron drip-line, until it reaches the zero line.

In the regions with the magic numbers ($N = 50, 82$ and 126), we see that the λ_n values of these numbers are higher than (sharp drop) in the neighboring regions, and this property can be observed, which appears in Fig. 6, *c*, as prominent peaks. The positive energy values of λ_n are concentrated in the regions of nuclei with $12 \leqslant N \leqslant 94$, $128 \leqslant N \leqslant 136$ and $186 \leqslant N \leqslant 200$, whereas the positive energy values of λ_p are focused in the regions with $2 \leqslant N \leqslant 154$, as can be seen in Fig. 6, *c, d* for the neutron and proton Fermi energies, respectively. The λ_p values of the isotopic chain are more regular in the process of decreasing with the increasing of the neutron number N, as is shown in Fig. 6, *d*.

The calculated results for E^n_Δ, E^p_Δ, λ_n, and λ_p with the SKI3 force have been presented as a function of the proton (Z) number, as is shown in Fig. 7, *a, b, c, d*, respectively. In contrast to Fig. 6, *a*, the regions with the magic numbers ($N = 28, 50$ and 82) have large values of E^n_Δ and appear as peaks. Remarkably, the regions of those nuclei which are located between the magic numbers have low values of E^n_Δ, as is shown in Fig. 7, *a*, while that regions between the magic numbers $N = 28, 50$, and 82 have large values of the proton pairing energy E^p_Δ, as is seen in Fig. 7, *b*. The positive energy values of λ_n are concentrated in the regions of nuclei with $4 \leqslant Z \leqslant 44$, $54 \leqslant Z \leqslant 62$ and $80 \leq Z \leq 88$. The positive energy values of λ_p are concentrated in the regions with $6 \leqslant Z \leqslant 110$, as can be seen in Fig. 7, *c, d* for λ_n and λ_p, respectively. Both λ_n and λ_p for the isotopic chain are more regular in the process of decreasing with the increasing of the proton number Z.

5. Conclusions

In this work, the ground-state properties for about 2095 even-even nuclei ($2 \leqslant Z \leqslant 110$) over a wide range of isotopes ($2 \leqslant N \leqslant 236$, $4 \leqslant A \leqslant 346$) of the whole nuclear chart have been systematically studied by using the Skyrme (SKI3) force with the mixed volume-surface pairing in the framework of the Hartree–Fock–Bogoliubov theory. The calculated ground-state properties include the proton pairing gap, neutron and proton pairing energies, and neutron and proton Fermi energies. The calculated proton pairing gaps have been compared with the experimental proton pairing gaps using the formulas $\Delta^{(3)}$, $\Delta^{(4)}$, and $\Delta^{(5)}$ and are compared with the proton pairing gaps in the Lipkin–Nogami model. We conclude that the Skyrme (SKI3) force with the mixed volume-surface pairing can be successfully used for describing the proton pairing gap, neutron and proton pairing energies, and neutron and proton Fermi energies of the investigated nuclei, in particular, the neutron-rich nuclei and the exotic nuclei near the neutron drip-line. Moreover, the calculated proton pairing gaps show a good agreement with experimental data with the use of the difference-point formulas $\Delta^{(3)}$, $\Delta^{(4)}$, and $\Delta^{(5)}$ and with the Lipkin–Nogami model. Finally, we have obtained a regular agreement of the calculated proton pairing gaps with the difference-point formulas (in particular, with $\Delta^{(3)}$ and $\Delta^{(4)}$) for $20 \leqslant Z \leqslant 110$, $20 \leqslant N \leqslant 170$, except for some nuclei (with red color in the chart of nuclei), as well as the agreement of the calculated proton pairing gaps with those in the Lipkin–Nogami model $26 \leqslant Z \leqslant 110$, $26 \leqslant N \leqslant 236$, except for some nuclei (with yellow color in the chart of nuclei).

1. X. Yu Liu, C. Qi. PairDiag: An exact diagonalization program for solving general pairing Hamiltonians. *Comput. Phys. Commun.* **259**, 107349 (2021).
2. M. Bender, K. Rutz, P.-G. Reinhard, J.A. Maruhn. Pairing gaps from nuclear mean-fieldmo dels. *Eur. Phys. J. A* **8**, 59 (2000).
3. V. Thakur, P. Kumar, S. Thakur, S. Thakur, V. Kumar, S.K. Dhiman. Microscopic study of the shell structure evolution in isotopes of light to middle mass range nuclides. *Nucl. Phys. A* **1002**, 121981 (2020).
4. T.-T. Sun, L. Qian, C. Chen, P. Ring, Z.P. Li. Green's function method for the single-particle resonances in a deformed Dirac equation. *Phys. Rev. C* **101**, 014321 (2020).
5. N.J. Abu Awwad, H. Abusara, S. Ahmad. Ground state properties of Zn, Ge, and Se isotopic chains in covariant density functional theory. *Phys. Rev. C* **101**, 064322 (2020).
6. B. Dey, S-S. Wang, D. Pandit, S. Bhattacharya, X-G. Cao, W-B. He, Y-G. Ma, N.Q. Hung, N.D. Dang. Exotic nuclear shape due to cluster formation at high angular momentum. *Phys. Rev. C* **102**, 031301(R) (2020).
7. Z. Matheson, S.A. Giuliani, W. Nazarewicz, J. Sadhukhan, N. Schunck. Cluster radioactivity of $118^{294}\mathrm{Og}_{176}$. *Phys. Rev. C* **99**, 041304(R) (2019).

8. P. Moller, J.R. Nix. Nuclear pairing models. *Nucl. Phys. A* **536**, 20 (1992).
9. S. Mizutori, J. Dobaczewski, G.A. Lalazissis, W. Nazarewicz, P.-G. Reinhard. Nuclear skins and halos in the mean-field theory. *Phys. Rev. C* **61**, 044326 (2000).
10. P. Ring, P. Schuck. *The Nuclear Many-Body Problem* (Springer-Verlag, 1980) [ISBN: 0-387-09820-8].
11. M.V. Stoitsov, J. Dobaczewski, W. Nazarewicz, P. Ring. Axially deformed solution of the Skyrme-Hartree-Fock-Bogoliubov equations using the transformed harmonic oscillator basis. The program HFBTHO (v1.66p). *Comput. Phys. Commun.* **167**, 43-63 (2005).
12. M.V. Stoitsov, N. Schunck, M. Kortelainen, N. Michel, H. Nam, E. Olsen, J. Sarich, S. Wild. Axially deformed solution of the Skyrme–Hartree–Fock–Bogoliubov equations using the transformed harmonic oscillator basis (II) HFBTHO v2.00d: A new version of the program. *Comput. Phys. Commun.* **184**, 1592 (2013).
13. M. Bender, P.-H. Heenen, P.-G. Reinhard. Self-consistent mean-field models for nuclear structure. *Rev. Mod. Phys* **75**, 121 (2003).
14. J. Dobaczewski, H. Flocard, J. Treiner. Hartree–Fock–Bogolyubov description of nuclei near the neutron-Drip Line. *Nucl. Phys. A* **422**, 103-139 (1984).
15. A. Bulgac. Hartree–Fock–Bogoliubov approximation for finite systems. IPNE FT-194-1980, Bucharest (arXiv: nucl-th/9907088) (1999).
16. S.A. Changizi, C. Qi, R. Wyss. Empirical pairing gaps, shell effects, and di-neutron spatial correlation in neutron-rich nuclei. *Nucl. Phys. A* **940**, 210 (2015).
17. J. Bardeen, L.N. Cooper, J.R. Schrieffer. Theory of Superconductivity. *Phys. Rev.* **108**, 1175 (1957).
18. J.A. Sheikh, P. Ring. Symmetry-projected Hartree–Fock–Bogoliubov equations. *Nucl. Phys. A* **665**, 71 (2000).
19. N. Schunck, M.V. Stoitsov, W. Nazarewicz, N. Nikolov. Large-Scale Calculations in Odd-Mass Nuclei. *AIP Conf. Proceedings* **1128**, 40 (2009).
20. A.H. Taqi, M.A. Hasan. Ground-State properties of even-even nuclei from He ($Z = 2$) to Ds ($Z = 110$) in the framework of Skyrme–Hartree–Fock–Bogoliubov theory. *Arab. J. Sci. Eng.* **47**, 761 (2022).
21. S.A. Changizi, C. Qi. Density dependence of the pairing interaction and pairing correlation in unstable nuclei. *Phys. Rev. C* **91**, 024305 (2015).
22. S.A. Changizi, C. Qi. Odd-even staggering in neutron drip line nuclei. *Nucl. Phys. A* **951**, 97 (2016).
23. P.-G. Reinhard, H. Flocard. Nuclear effective forces and isotope shifts. *Nucl. Phys. A* **584**, 467 (1995).
24. P. Moller, M.R. Mumpower, T. Kawano, W.D. Myers. Nuclear properties for astrophysical and radioactive-ion-beam applications (II). *Atom. Data Nucl. Data Tab* **125**, 1 (2019).
25. K. Zhang *et al.* (DRHBc Mass Table Collaboration). Deformed relativistic Hartree–Bogoliubov theory in continuum with a point-coupling functional: Examples of even-even Nd isotopes. *Phys. Rev. C* **102**, 024314 (2020).
26. X.W. Xia, Y. Lim, P.W. Zhao, H.Z. Liang, X.Y. Qu, Y. Chen, H. Liu, L.F. Zhang, S.Q. Zhang, Y. Kim, J. Meng. The limits of the nuclear landscape explored by the relativistic continuum Hartree–Bogoliubov theory. *Atom. Data Nucl. Data Tab.* **121–122**, 1 (2016).
27. A.H. Taqi, M.A. Hasan. Skyrme–Hartree–Fock–Bogoliubov calculations of even and odd neutron-rich Mg isotopes. *Ukr. J. Phys* **66** (11), 928 (2021).
28. Y. El Bassem, M. Oulne. Hartree–Fock–Bogoliubov calculation of ground state properties of even-even and odd Mo and Ru isotopes. *Nucl. Phys. A* **957**, 22 (2017).
29. W. Satula, J. Dobaczewski, W. Nazarewicz. Odd-even staggering of nuclear masses: Pairing or shape effect? *Phys. Rev. Lett.* **81**, 3599 (1998).
30. S.J. Krieger, P. Bonche, H. Flocard, P. Quentin, M.S. Weiss. An improved pairing interaction for mean field calculations using skyrme potentials. *Nucl. Phys. A* **517**, 275 (1990).
31. S. Cwiok, J. Dobaczewski, P.-H. Heenen, P. Magierski, W. Nazarewicz. Shell structure of the superheavy elements. *Nucl. Phys. A* **611**, 211 (1996).
32. A. Bohr, B.R. Mottelson. *Nuclear Structure Volume I: Single-Particle Motion* (World Scientific publishing Co. Pte. Ltd, 1998) [ISBN: 10 981-02-3979-3].
33. A.H. Taqi, P.F. Mahmood. Nuclear structure investigation of even-even isotopes from ^{94}Sn to ^{272}Pb. *Iran. J. Sci. Technol. Trans. Sci.* **45**, 2149 (2021).
34. A.H. Taqi, S.M. Qatal. Nuclear structure of samarium isotopes using skyrme and gogny Hartree–Fock–Bogoliubov method. *Iran. J. Sci. Technol. Trans. Sci.* **46**, 967 (2022).

Received 28.07.23

М.А. Хасан, А.Х. Такі

ВЛАСТИВОСТІ ЗМІШАНОГО ОБ'ЄМНО-ПОВЕРХНЕВОГО ДВІЙКУВАННЯ ПРОТОНІВ І НЕЙТРОНІВ В ТЕОРІЇ ХАРТРІ–ФОКА–БОГОЛЮБОВА

Досліджено властивості двійкування протонів і нейтронів та їхні енергії Фермі в області між протонною і нейтронною лініями стабільності. Щоб отримати більш точну масову формулу у випадку сили Скірма (SKI3), ми застосували модель Скірма–Хартрі–Фока–Боголюбова. В рамках цієї моделі, для змішаного об'ємно-поверхневого утворення пар протонів і нейтронів розраховано щілину для двійкування протонів в основному стані, енергії двійкування та енергії Фермі для близько 2095 парно-парних ядер у діапазоні $2 \leqslant Z \leqslant 110$ і $2 \leqslant N \leqslant 236$. Ми співставили результати розрахунків щілин для двійкування протонів з експериментальними даними, використовуючи різницево-точкові формули $\Delta^{(3)}$, $\Delta^{(4)}$ та $\Delta^{(5)}$, і з результатами моделі Ліпкіна–Ногамі. Зокрема, нам вдалося отримати цілком прийнятні результати для ядер, багатих на нейтрони, та екзотичних ядер біля нейтронної лінії стабільності.

Ключові слова: теорія Скірма–Хартрі–Фока–Боголюбова, щілина протонного двійкування, енергія двійкування, енергія Фермі.